

Ford, H.L., and Raymo, M.E., 2020, Regional and global signals in seawater $\delta^{18}\text{O}$ records across the mid-Pleistocene transition: *Geology*, v. 48, <https://doi.org/10.1130/G46546.1>

APPENDIX

Site 1208

Based on sample availability, samples were taken at ~7, 10, and 20 cm intervals from 40-53, 21.7-24, and 24-40/53-87 mbsf, respectively. This equates to a temporal resolution of 1.4 to 3.7 kyr. As site 1208 is a single hole, we constructed a “re-compressed” depth, as in Venti and Billups (2012):

$$((\text{reported depth} - \text{core-top depth}) * (100 / \% \text{ core recovered}) + \text{core-top depth})$$

Prob-stack and LR04

In the years since the publication of the $\delta^{18}\text{O}_{\text{benthic}}$ LR04 stack (Lisiecki and Raymo, 2005) researchers have produced new $\delta^{18}\text{O}_{\text{benthic}}$ records. An updated version of LR04 is Prob-stack (Ahn et al., 2017). Prob-stack includes 180 $\delta^{18}\text{O}_{\text{benthic}}$ globally distributed records whereas LR04 included 57 $\delta^{18}\text{O}_{\text{benthic}}$ records. Prob-stack and LR04 are similar in structure (**Data Repository Figure 1**).

Minor Elemental Analyses

Uvigerina spp. was used to reconstruct bottom water temperature at Ocean Drilling Program Site 1208. Marine sediment samples were washed and picked for *Uvigerina* spp. specimens from the > 250 μm size fraction. Prior to analysis, 6-12 *Uvigerina* spp. specimens were crushed, washed using MilliQ water and methanol, and reductively and oxidatively cleaned. Prepared samples were analyzed for minor and trace elements on the Thermo Scientific iCAP-Q inductively coupled plasma mass spectrometer (ICP-MS) at the Lamont-Doherty Earth Observatory and Rutgers University. Long-term precision of a liquid consistency standard is ~1-

2% . The pooled standard deviation of the replicate *Uvigerina* spp. Mg/Ca determinations is 0.056 mmol/mol. Al, Fe and Mn were used to screen for contamination (**Data Repository Figure 2 and 3**; n = 4 samples were eliminated because the Mn/Ca or Fe/Ca values were >350 mmol/mol or $\mu\text{mol/mol}$, respectively). No preservation biases are observed in percent coarse fraction or lightness as a proxy for percent CaCO_3 (**Data Repository Figure 4**).

Converting to Bottom Water Temperature and $\delta^{18}\text{O}_{\text{seawater}}$

PSU Solver (Thirumalai et al., 2016) was used to estimate bottom water temperature and $\delta^{18}\text{O}_{\text{seawater}}$ (**Data Repository Figure 5, 6 and 7**). PSU Solver uses a Monte Carlo simulation ($n = 1000$) to propagate errors on bottom water temperature and $\delta^{18}\text{O}_{\text{sw}}$ estimates.

The following equations were used:

(1) $\text{Mg/Ca} = 1.0 + (0.1 \cdot \text{BWT})$ from (Elderfield et al., 2010; Elderfield et al., 2012) with oxidative cleaning only

(2) $\text{Mg/Ca} = 0.9 + (0.1 \cdot \text{BWT})$ modified from (Elderfield et al., 2010; Elderfield et al., 2012) with oxidative and reductive cleaning (Woodard et al., 2014; Ford et al., 2016)

(3) $\text{Mg/Ca} = 1.16 + (0.15 \cdot T)$ from (Sosdian and Rosenthal, 2009)

(4) $\text{Temperature} = 16.9 - 4.0 \cdot (\delta^{18}\text{O}_{\text{carbonate}} - \delta^{18}\text{O}_{\text{sw}} + 0.27)$ from (Shackleton, 1974; Kim and O'Neil, 1997; Elderfield et al., 2010; Elderfield et al., 2012)

Bottom water temperature for *Uvigerina* spp. was estimated using equation 1 and equation 2 for ODP Site 1123 and Site 1208, respectively. For the multi-species bottom water temperature reconstruction at DSDP Site 607, equation 2 was used for *Uvigerina* spp. and

equation 3 was used *Cibicidoides wuellerstorfi* and *Oridorsalis umbonatus*. The Mg/Ca uncertainty for *Uvigerina* spp. is 0.06 mmol/mol and 0.16 mmol/mol for *Cibicidoides wuellerstorfi* and *Oridorsalis umbonatus*. The $\delta^{18}\text{O}_{\text{carbonate}}$ uncertainty is 0.06 per mill. The age model uncertainty is 1 kyrs.

Constructing the $\delta^{18}\text{O}_{\text{seawater}}$ Stack

Using the $\delta^{18}\text{O}_{\text{sw}}$ estimates from ODP Sites 1123 and 1208 and DSDP Site 607 from PSU Solver (**Data Repository Figure 8**), we created a $\delta^{18}\text{O}_{\text{sw}}$ stack. First, the $\delta^{18}\text{O}_{\text{sw}}$ estimates for each site were interpolated the records to an even 3-kyr interval (across the 338-1450 ka interval where all three records ≤ 3 kyr resolution, **Data Repository Figure 9**). During the 338 – 1450 ka interval Sites 607, 1123, and 1208 have a ~ 3.0 kyr, 2.7 kyr, and 1.0 kyr sampling resolution, respectively. Each record was then bootstrapped to estimate error ($n = 1000$, **Data Repository Figure 10**). The interpolated means the bootstrapped error estimates were then averaged to create the mean and error estimate of the $\delta^{18}\text{O}_{\text{sw}}$ stack (**Data Repository Figure 11**).

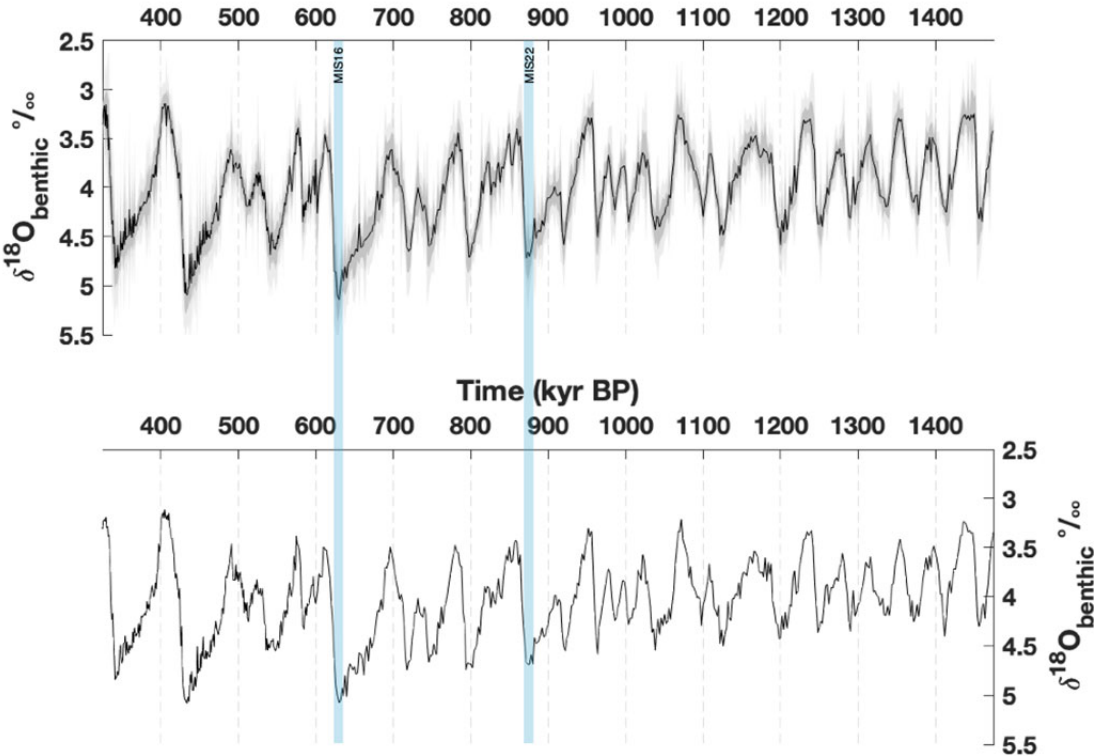
Wavelet analyses of the individual $\delta^{18}\text{O}_{\text{sw}}$ and $\delta^{18}\text{O}_{\text{sw}}$ stack

Continuous 1-D wavelet transforms were calculated using the Matlab® function cwt (Data Repository Figure 12). The Probstack has strong 41- and 100-kyr signal. The d18Osw records have weak 41-kyr signal and 100-kyr signal that begins ~ 900 kyr and becomes stronger at ~ 600 kyr.

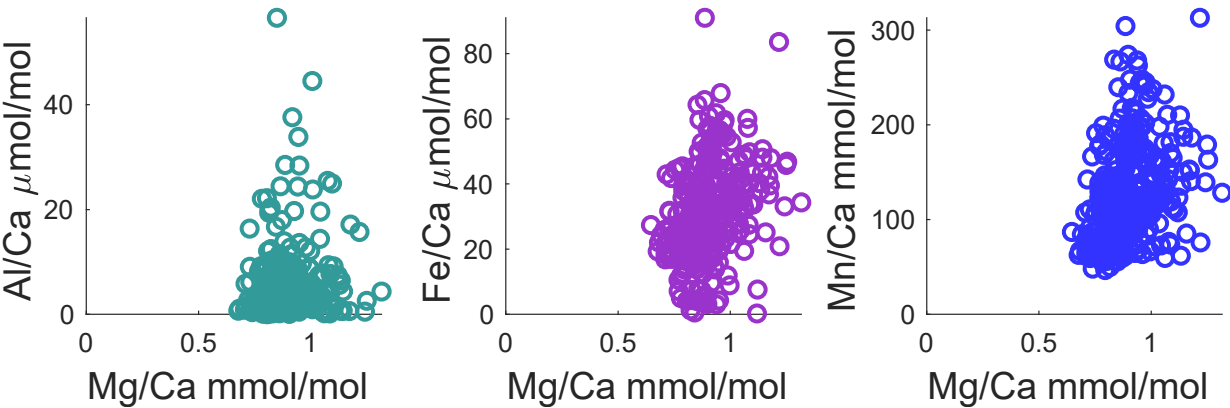
Data Set

2020037_Data Set.xlsx

69 **Data Repository Figure 1:** Prob-stack (top) and LR04 (bottom). Error envelopes: dark grey =
70 1σ , light grey = 2σ).



72 **Data Repository Figure 2:** Scatter plots of Mg, Al, Fe and Mn.

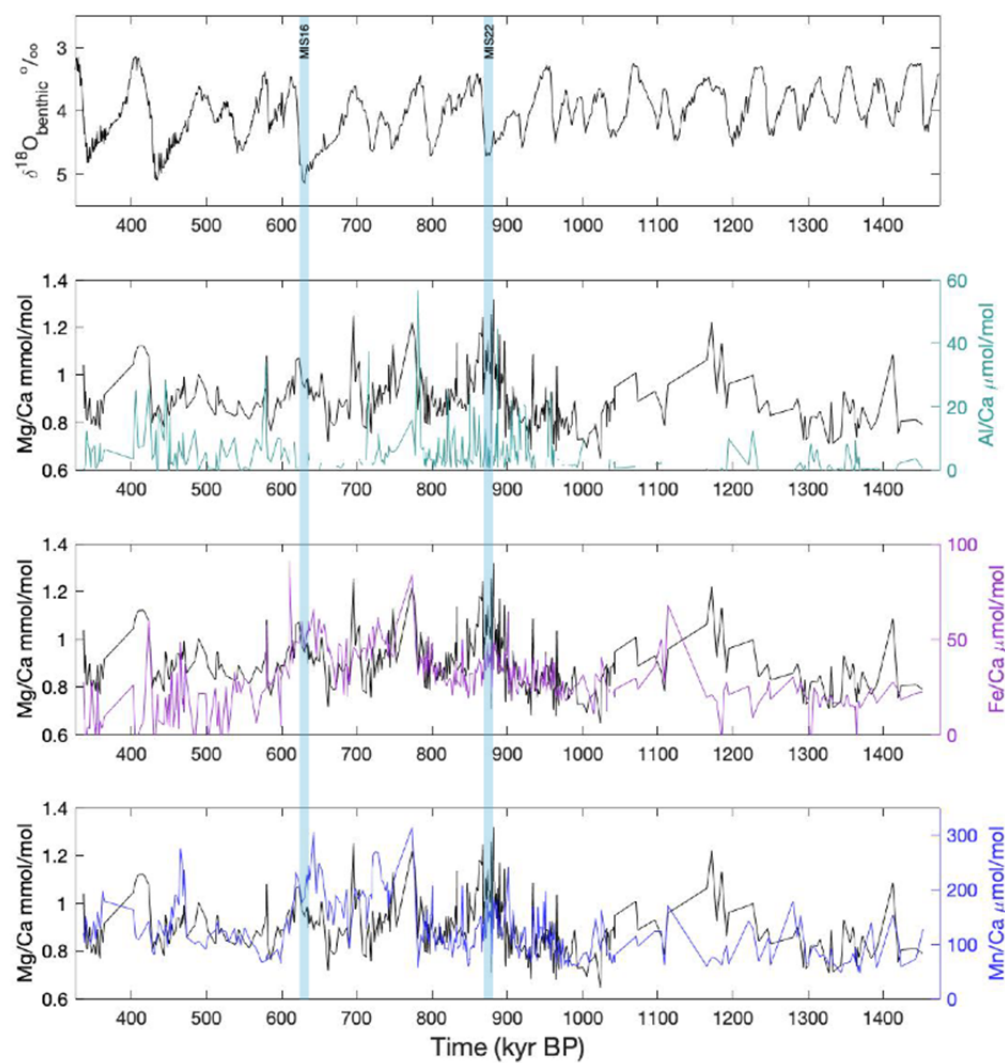


73

74

75

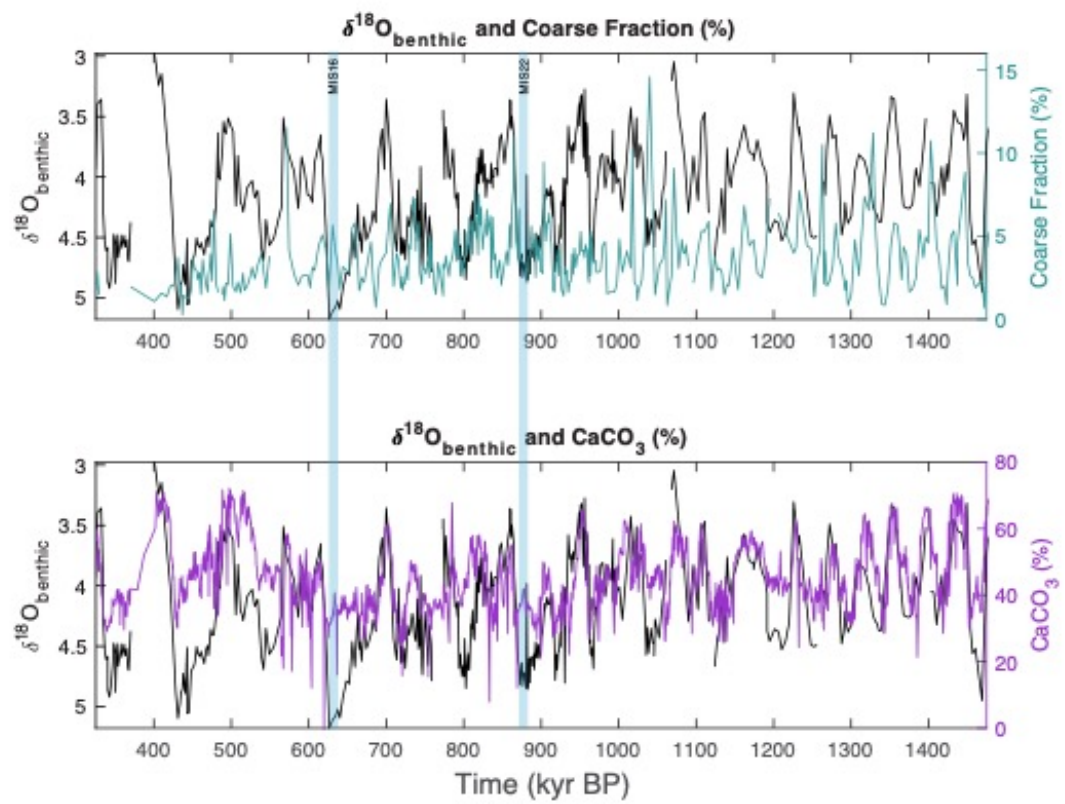
76 **Data Repository Figure 3: Time series plots of Mg (black), Al, Fe and Mn.**



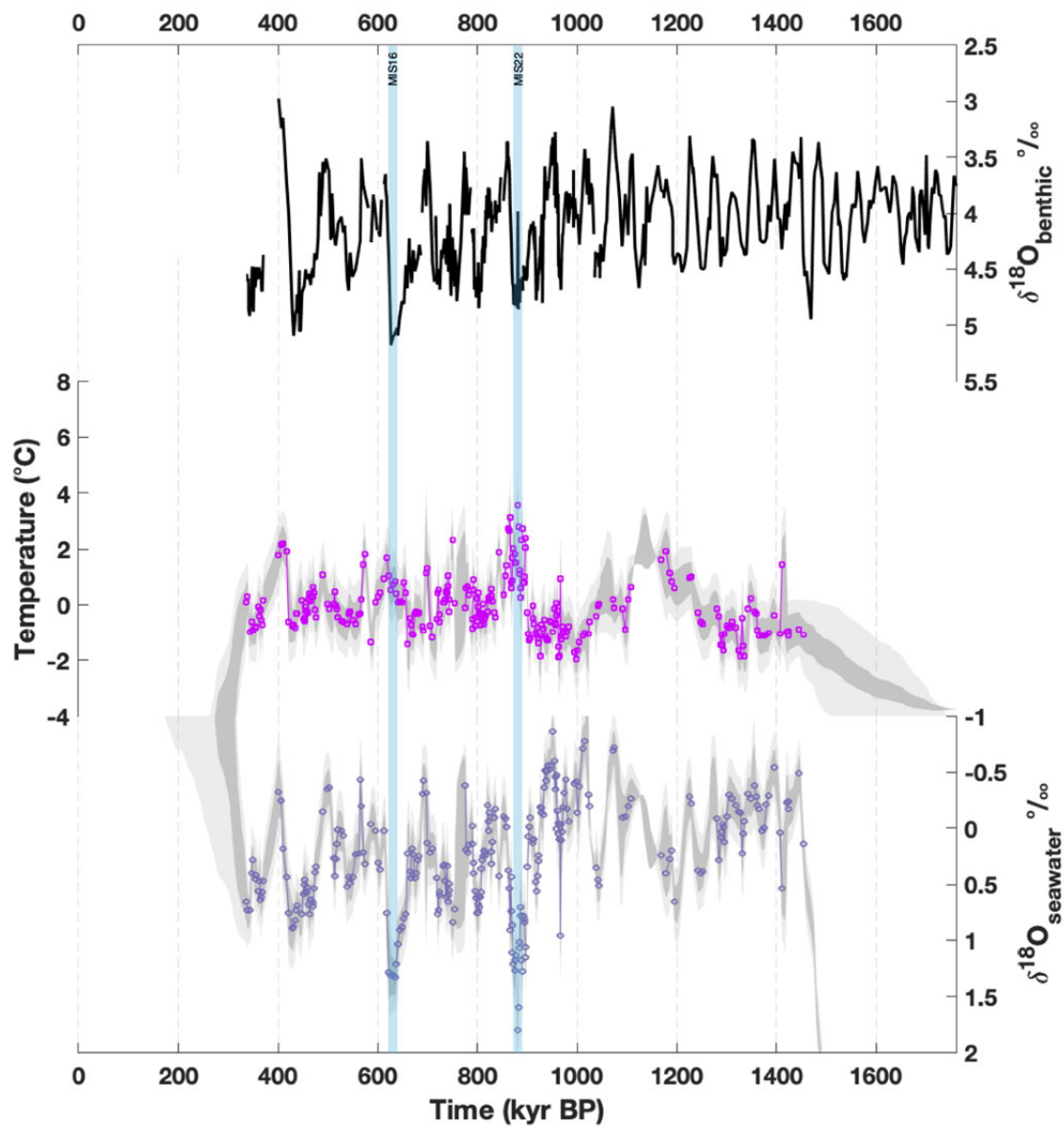
77

78

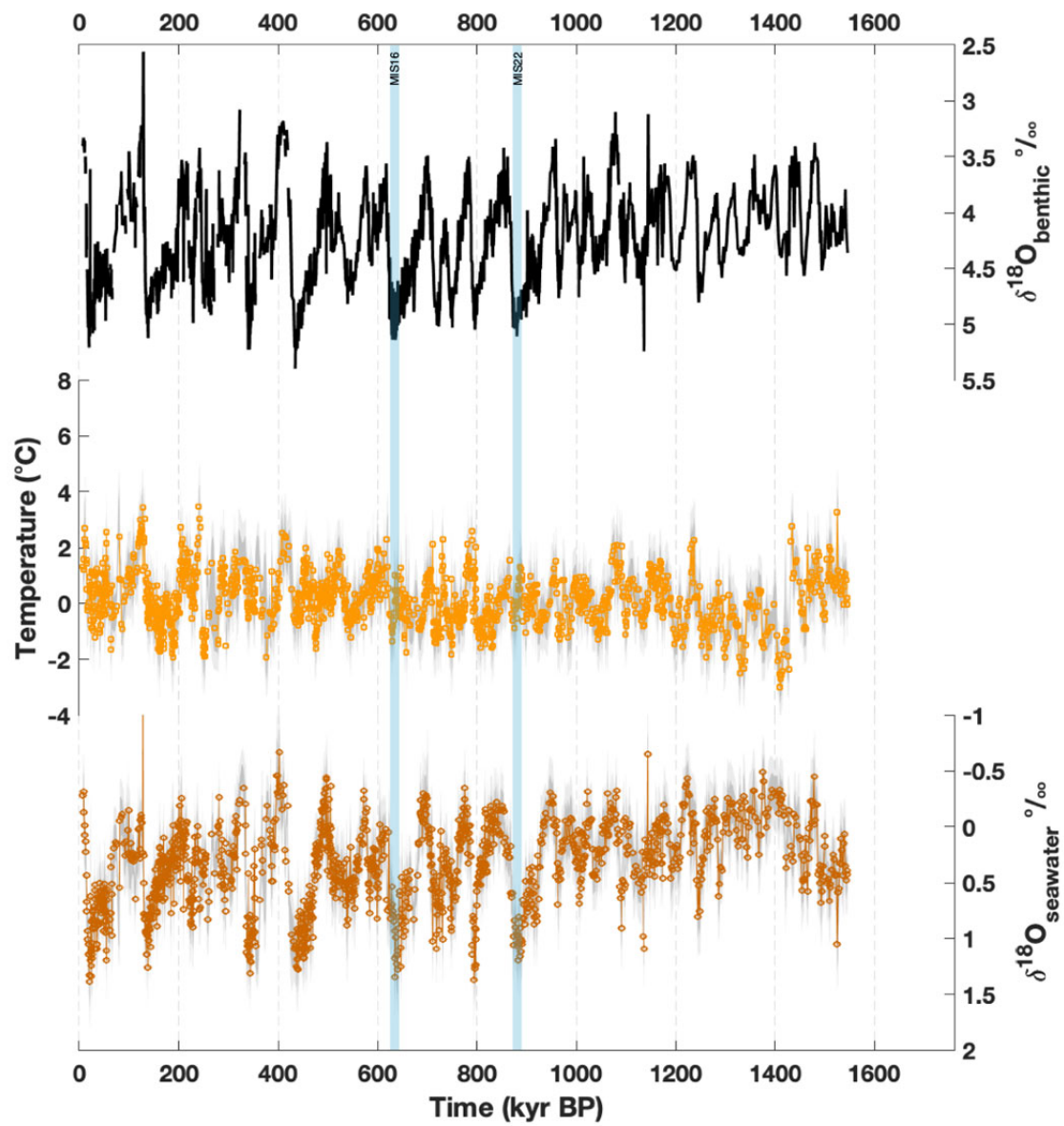
79 **Data Repository Figure 4:** Time series plots of Site 1208 $\delta^{18}\text{O}_{\text{benthic}}$ (black) and Coarse Fraction
80 (%) and CaCO_3 (%) showing no obvious preservation bias in the Site 1208 Mg/Ca record.



Data Repository Figure 5: N. Pacific ODP Site 1208 $\delta^{18}\text{O}_{\text{benthic}}$, Mg/Ca derived temperature and $\delta^{18}\text{O}_{\text{seawater}}$. Using Monte Carlo simulations, PSU Solver (Thirumalai et al., 2016) generated error envelopes (dark grey = 1σ , light grey = 2σ) on temperature and $\delta^{18}\text{O}_{\text{seawater}}$.



89 **Data Repository Figure 6:** S. Pacific ODP Site 1123 $\delta^{18}\text{O}_{\text{benthic}}$, Mg/Ca derived temperature and
90 $\delta^{18}\text{O}_{\text{seawater}}$. Using Monte Carlo simulations, PSU Solver (Thirumalai et al., 2016) generated error
91 envelopes (dark grey = 1σ , light grey = 2σ) on temperature and $\delta^{18}\text{O}_{\text{seawater}}$.

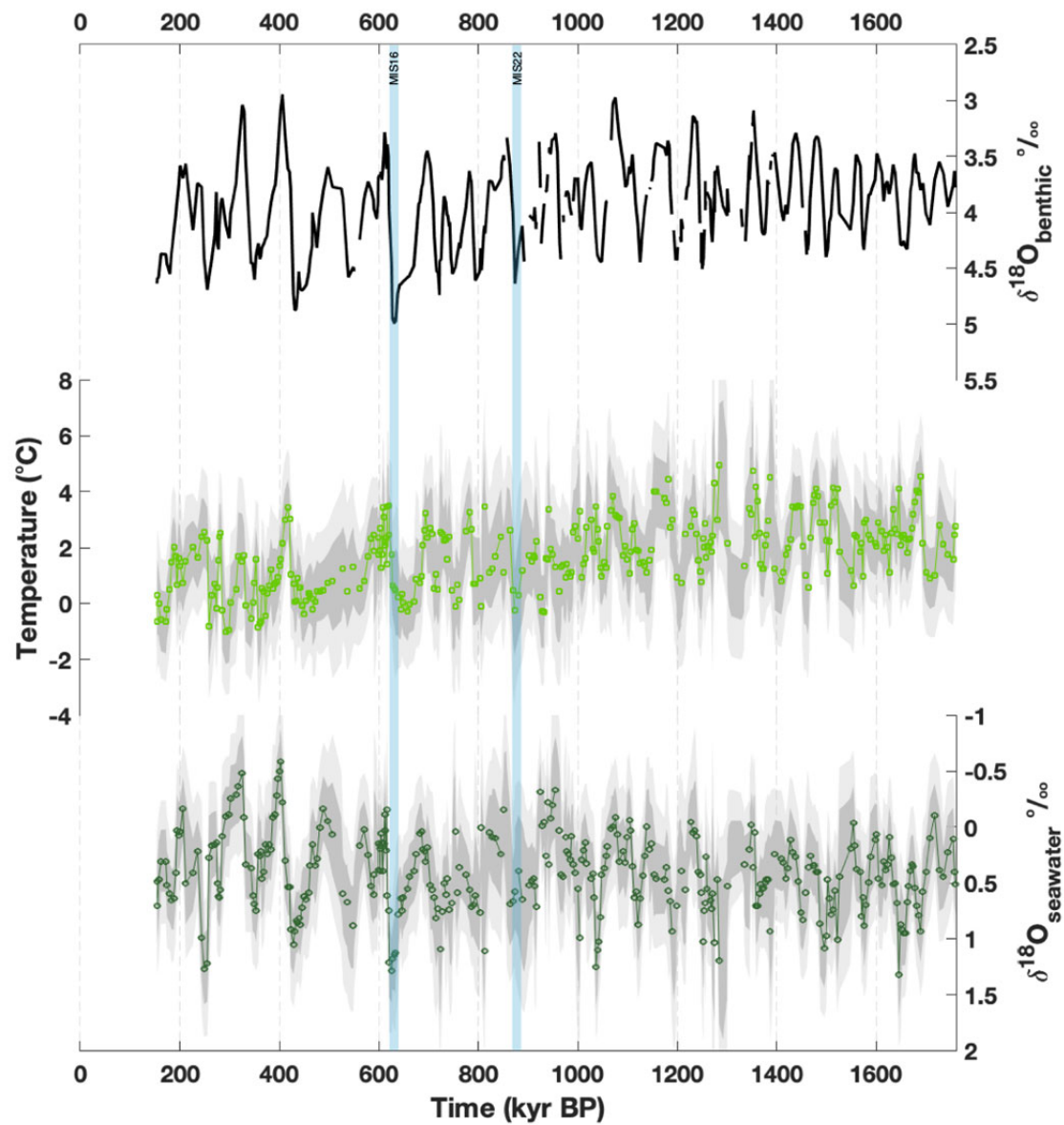


92

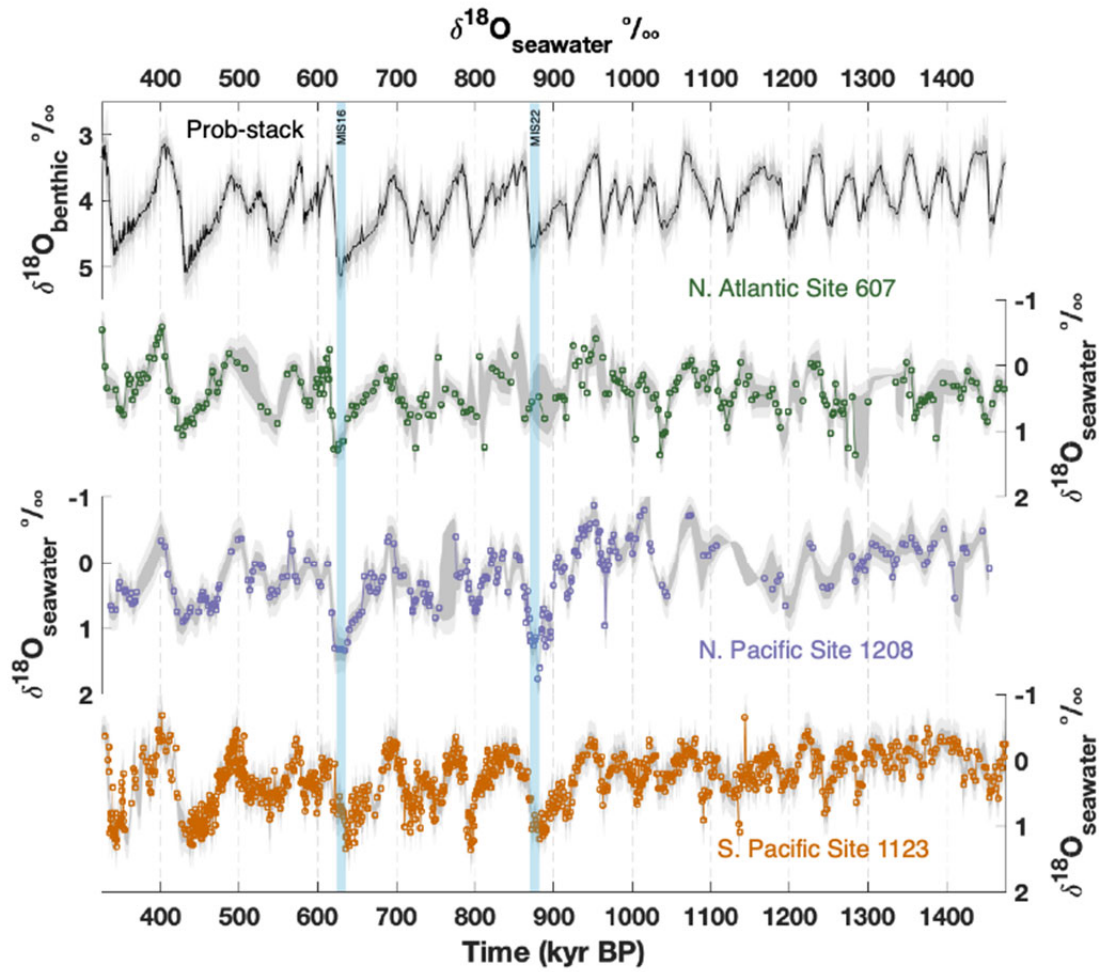
93

94

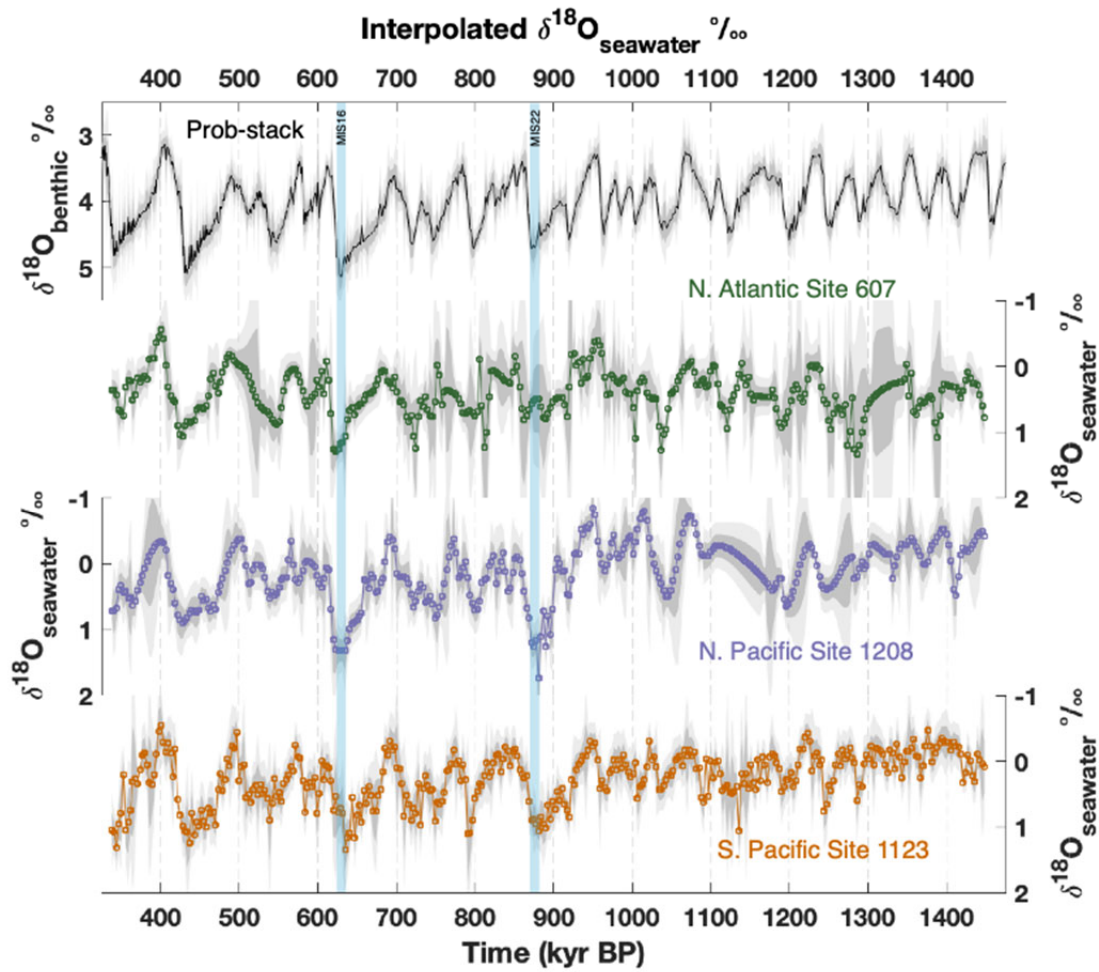
Data Repository Figure 7: N. Atlantic DSDP Site 607 $\delta^{18}\text{O}_{\text{benthic}}$, Mg/Ca derived temperature and $\delta^{18}\text{O}_{\text{seawater}}$. Using Monte Carlo simulations, PSU Solver (Thirumalai et al., 2016) generated error envelopes (dark grey = 1σ , light grey = 2σ) on temperature and $\delta^{18}\text{O}_{\text{seawater}}$.



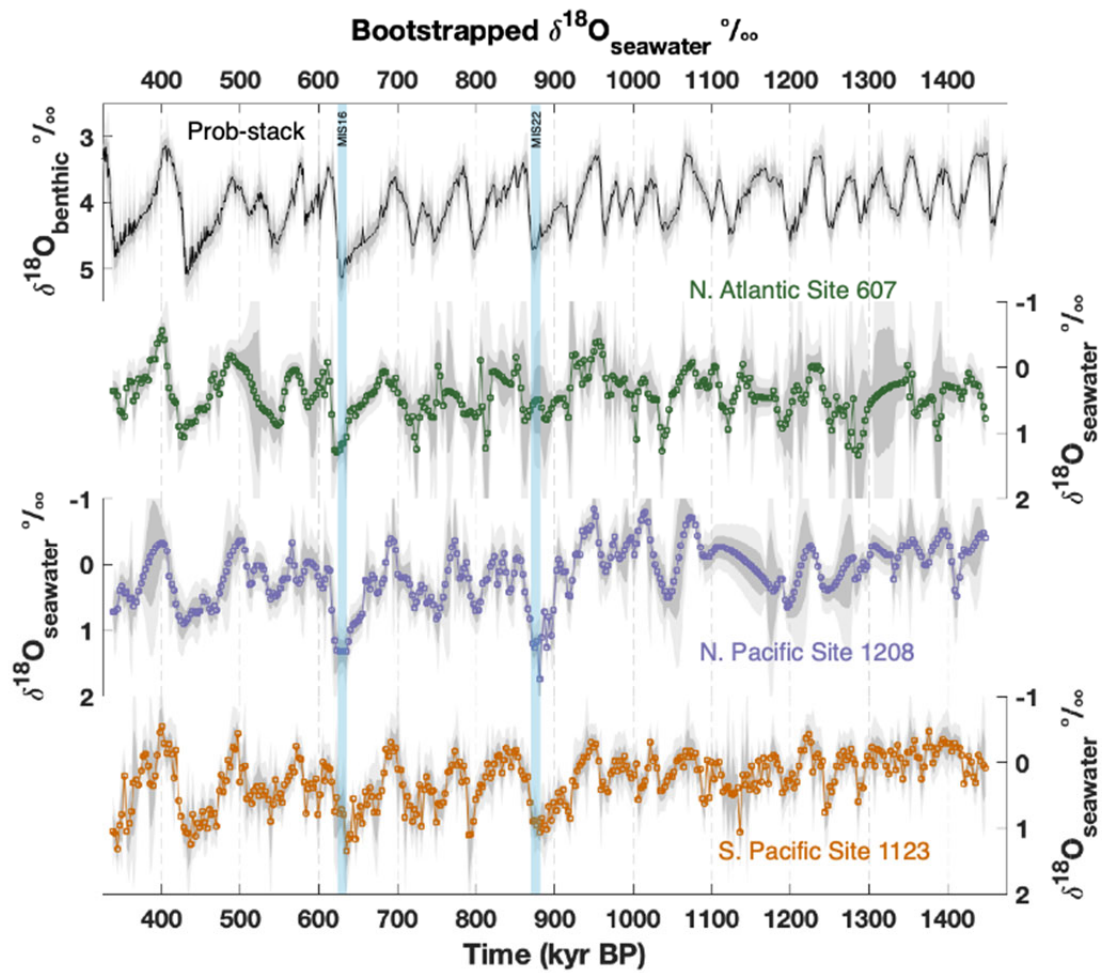
100 **Data Repository Figure 8:** Prob-stack and $\delta^{18}\text{O}_{\text{seawater}}$ records from ODP 1208 and 1123 and
101 DSDP 607. Error envelopes: dark grey = 1σ , light grey = 2σ).



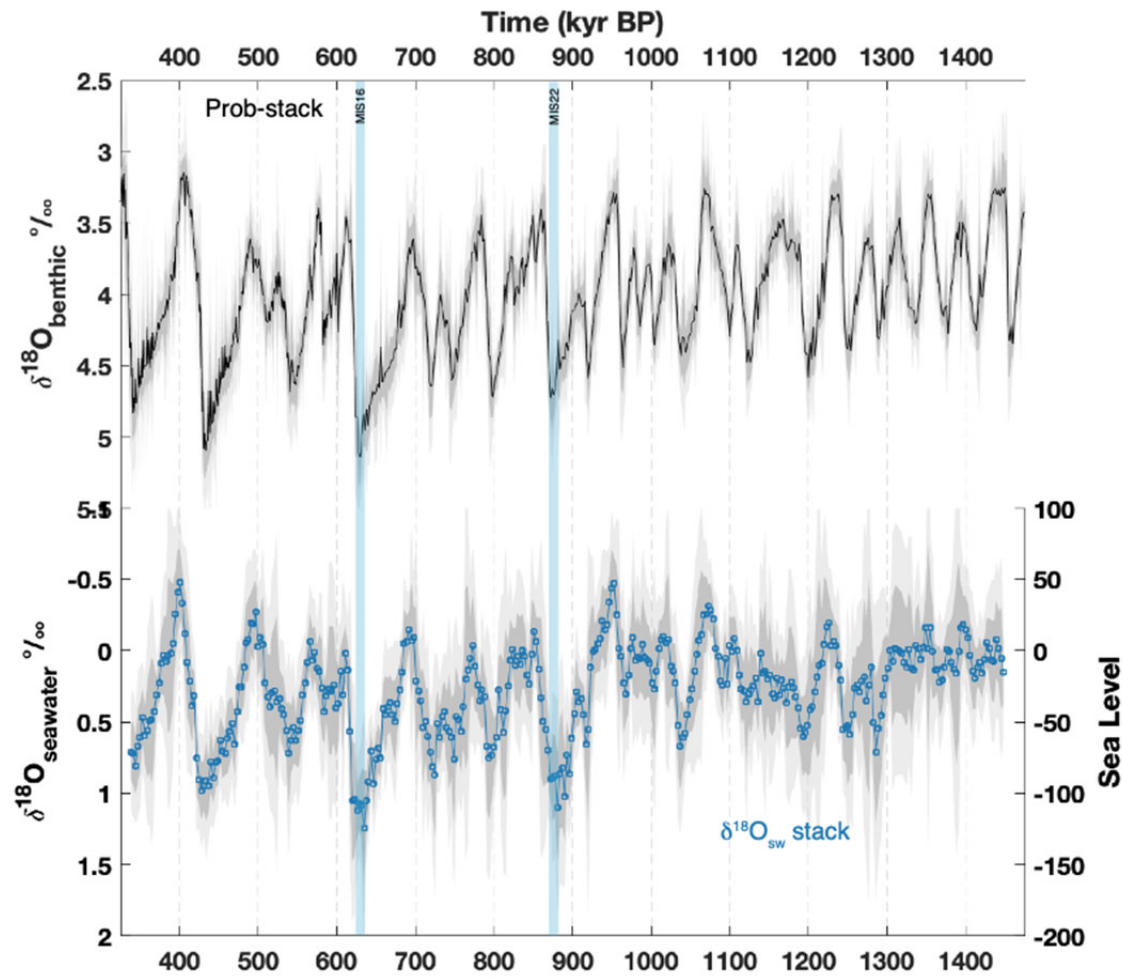
104 **Data Repository Figure 9:** Prob-stack and interpolated $\delta^{18}\text{O}_{\text{seawater}}$ records from ODP 1208 and
105 1123 and DSDP 607. Error envelopes: dark grey = 1σ , light grey = 2σ).



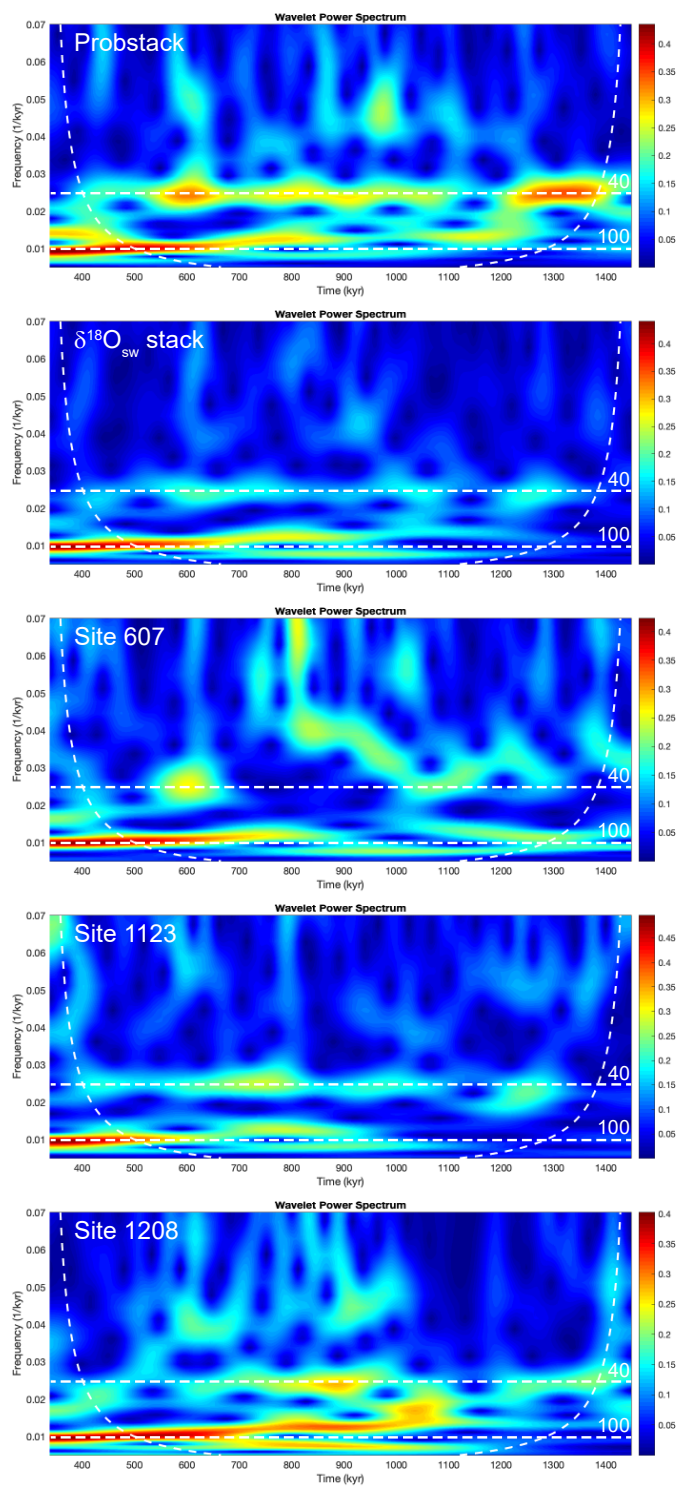
108 **Data Repository Figure 10:** Prob-stack and bootstrapped $\delta^{18}\text{O}_{\text{seawater}}$ records from ODP 1208
109 and 1123 and DSDP 607. Error envelopes: dark grey = 1σ , light grey = 2σ).



112 **Data Repository Figure 11:** Prob-stack and $\delta^{18}\text{O}_{\text{sw}}$ stack. Error envelopes: dark grey = 1σ , light
113 grey = 2σ).



117 **Data Repository Figure 12:** Wavelet analyses of Prob Stack, $\delta^{18}\text{O}_{\text{sw}}$ stack, and $\delta^{18}\text{O}_{\text{sw}}$ records
 118 from Sites 607, 1123 and 1208.



- 120 Ahn, S., Khider, D., Lisiecki, L.E., and Lawrence, C.E., 2017, A probabilistic Pliocene–
121 Pleistocene stack of benthic $\delta^{18}\text{O}$ using a profile hidden Markov model: Dynamics and
122 Statistics of the Climate System, v. 2, no. 1, p. 91–16, doi: 10.1093/climsys/dzx002.
- 123 Elderfield, H., Ferretti, P., Greaves, M., Crowhurst, S., McCave, I.N., Hodell, D., and
124 Piotrowski, A.M., 2012, Evolution of Ocean Temperature and Ice Volume Through the Mid-
125 Pleistocene Climate Transition: Science, v. 337, no. 6095, p. 704–709, doi:
126 10.1126/science.1221294.
- 127 Elderfield, H., Greaves, M., Barker, S., Hall, I.R., Tripathi, A., Ferretti, P., Crowhurst, S., Booth,
128 L., and Daunt, C., 2010, A record of bottom water temperature and seawater $\delta^{18}\text{O}$ for the
129 Southern Ocean over the past 440kyr based on Mg/Ca of benthic foraminiferal *Uvigerina*
130 spp.: Quaternary Science Reviews, v. 29, no. 1, p. 160–169.
- 131 Ford, H.L., Soshian, S.M., Rosenthal, Y., and Raymo, M.E., 2016, Gradual and abrupt changes
132 during the Mid-Pleistocene Transition: Quaternary Science Reviews, v. 148, no. C, p. 222–
133 233, doi: 10.1016/j.quascirev.2016.07.005.
- 134 Kim, S., and O'Neil, J., 1997, Equilibrium and nonequilibrium oxygen isotope effects in
135 synthetic carbonates: Geochimica et Cosmochimica Acta, v. 61, p. 3461–3475.
- 136 Lisiecki, L.E., and Raymo, M.E., 2005, A Pliocene-Pleistocene stack of 57 globally distributed
137 benthic $\delta^{18}\text{O}$ records: Paleoceanography, v. 20, no. 1, p. PA1003, doi:
138 10.1029/2004PA001071.
- 139 Shackleton, N.J., 1974, Attainment of isotopic equilibrium between ocean water and the
140 benthonic foraminifera genus *Uvigerina*: Isotopic changes in the ocean during the last
141 glacial: Colloques Internationaux du C.N.R.S., p. 203–209.
- 142 Soshian, S., and Rosenthal, Y., 2009, Deep-Sea Temperature and Ice Volume Changes Across
143 the Pliocene-Pleistocene Climate Transitions: Science, v. 325, no. 5938, p. 306–310, doi:
144 10.1126/science.1169938.
- 145 Thirumalai, K., Quinn, T.M., and Marino, G., 2016, Constraining past seawater $\delta^{18}\text{O}$ and
146 temperature records developed from foraminiferal geochemistry: Paleoceanography, doi:
147 10.1002/(ISSN)1944-9186.
- 148 Venti, N.L., and Billups, K., 2012, Stable-isotope stratigraphy of the Pliocene–Pleistocene
149 climate transition in the northwestern subtropical Pacific: *Palaeogeography*,
150 *Palaeoclimatology*, *Palaeoecology*, v. 326 p. 54–65.
- 151 Woodard, S.C., Rosenthal, Y., Miller, K.G., Wright, J.D., Chiu, B.K., and Lawrence, K.T., 2014,
152 Antarctic role in Northern Hemisphere glaciation: Science, v. 346, no. 6211, p. 847–851,
153 doi: 10.1126/science.1255586.